RSC Advances

ROYAL SOCIETY OF CHEMISTRY

www.rsc.org/advances

Graphical Table of Contents

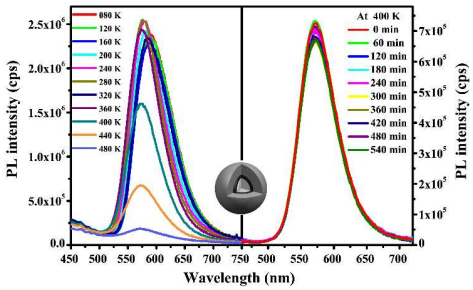

We reported the temperature-dependent photoluminescence of Mn:ZnCdS QDs with a high PL QY of 65% at 360 K.

Temperature-dependent Photoluminescence Properties of Mn:ZnCdS Quantum Dots

Jinju Zheng[1,2], *Sheng Cao*[2], *Lin Wang*[2], *Fengmei Gao*[2], *Guodong Wei*[2], *and Weiyou Yang*[2*]

[1]School of Mechanical Engineering, Ningbo University of Technology, Ningbo 315016, China.

[2] Institute of Materials, Ningbo University of Technology, Ningbo 315016, China.

Graphical Table of Contents

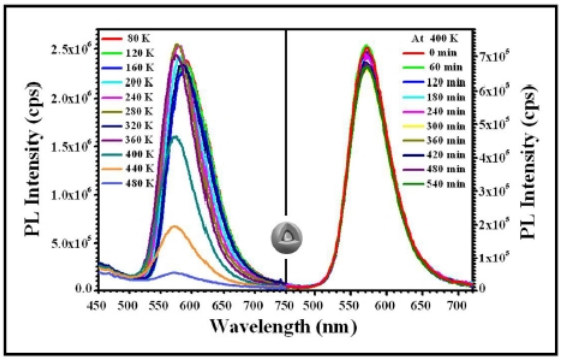

We reported the temperature-dependent photoluminescence of Mn:ZnCdS QDs with a high PL QY of 65% at 360 K.

* Corresponding author. weiyouyang@tsinghua.org.cn

Tel: +86-574-87080966, Fax: +86-574-87081221.

Abstract

With respect to the thermal effects being inevitable for the quantum dots (QDs) to be used in devices, the thermal stability of the QDs is considered as one of the crucial critically important issues for their practical application. In this work, we report the temperature-dependent photoluminescence (PL) of Mn:ZnCdS QDs, with the designed structure of MnS/ZnS/CdS, in the temperature range from 80 to 480 K. It is found that the highest PL quantum yield (QY) of the Mn:ZnCdS QDs can reach up to 65% even at the high temperature of 360 K. Meanwhile, the optical performance exhibits an excellent thermal stability, since the close-packed Mn:ZnCdS QDs and the QDs/organic blend films can keep 90% of its initial intensity at 400 K for a long time. The thermal quenching mechanism of Mn^{2+} ion emission is proposed. Present work suggests that the QDs with high PL QYs and enhanced thermal stabilities could be realized by blocking the nonradiative recombination centers with thick CdS shells.

Keywords: Temperature-dependent Photoluminescence, Thermal Stability, Mn^{2+} ions Doped Quantum Dot

1. Introduction

Quantum dots (QDs) have been considered as a revolutionizing material to be applied in next-generation luminescent and photovoltaic devices, due to their size-dependent properties, flexible solution processing, and higher photochemistry stability.[1-5] As compared to pure counterparts, the Mn^{2+} ion doped QDs have additional advantages of minimum self-quenching due to the large Stokes shift, long excited state lifetime, and enhanced thermal and chemical stabilities,[6-13] suggesting extensive applications in luminescent devices,[14-15] biological labels[16] and QD-sensitized solar cells.[17-18] Especially in recent years, doping Mn^{2+} ions in QDs has been proven to be a powerful strategy to extend the lifetime of charge carriers to boost the efficiency of QD-sensitized solar cells.[17-18] Owning to numerous efforts to the persistent improvement in the controllable synthesis of Mn^{2+} ions doped QDs[7,11,19-21] and deep understanding in their optoelectronic properties during the past decades,[8-11,22-24] the Mn^{2+} ions doped QDs become an very promising and excellent candidate materials to be used in the novel luminescent and photovoltaic devices with high performance.

Temperature-dependent photoluminescence properties of QDs are extensively interesting for QD-based devices,[25-27] such as photovoltaics,[28] phosphor converted light-emitting diodes (LEDs),[14,15] and luminescent concentrators.[29] These functional devices should be stable with high performance at elevated temperatures. However, the investigations on the thermal stability of the QDs remain limited.[30,31] Furthermore, in the reported works, significant thermal quenching of the QDs is often occurred even below 300 K. For examples, for Mn:ZnSe,[32] Mn:CdS[33] and Mn:ZnS QDs[34] which with low PL QY of less than 30%, there are higher than 50% loss of PL QY when the temperatures increased to room temperature. Although highly efficient Mn^{2+} ions emissions have been achieved in

Mn:ZnS,[35] Mn:ZnSe,[7,19] Mn:ZnSeS QDs[36] and Mn:ZnCdS[37] in recent years, there are scarcely works reported on the temperature-dependent optical properties of Mn^{2+} ions doped QDs.[30,38]

In this work, we reported the PL properties of Mn:ZnCdS QDs using time-resolved and temperature-dependent PL spectra in the range from 80 to 480 K. Nearly no evident variations in both the PL decay curves and integrated PL intensity of the Mn^{2+} ions emission were observed in the range from 80 to 360 K. The highest PL QY of 65% with an excellent thermal stability has been achieved in our synthesized Mn:ZnCdS QDs even at the high temperature of 360 K. In addition, the PL quenching mechanisms were explored by comparing the temperature-dependent integrated PL intensities and PL decay curves of Mn:ZnCdS QDs.

2. Experimental Section

The Mn^{2+} ions doped ZnCdS QDs (Mn:ZnCdS QDs) were synthesized by the nucleation-doping strategy, which was described detailed in the Supporting Information (The representative synthesis procedure for the Mn:ZnCdS QDs, ESI†), similar to our previous work.[37] A preformed MnS nanocrystal (NC) core was initially coated with the ZnS buffer layer and then further overcoating with CdS shell. The middle ZnS buffer layer of ~1 monolayer (ML) (Calculation of the ZnS buffer layer thicknesses, ESI†) was introduced to reduce the local strains derived from the lattice mismatch between MnS and CdS to obtain highly efficient Mn^{2+} ion emission. During the overcoating of ZnS/CdS shells on MnS cores, some of Mn^{2+} ions would diffuse from the MnS core to the ZnS/CdS shell due to the high activity of the small MnS cores and the high overcoating temperature, which leads to the formation of Mn:ZnCdS interface layers. The as-synthesized QDs exhibit an extremely high Mn^{2+} ion emission

with the QY of 70% (The PL quantum yield (QY) measurements, ESI†) at room temperature due to the fast energy transfer from the excitons in ZnCdS host to Mn^{2+} ions, which is similar to the Mn^{2+} ions doped ZnCdS QDs (so called Mn: ZnCdS QDs).

The inorganic/organic blend film of Mn^{2+} ions doped QD/1,3,5-tris(N-phenylbenz-imidazol-2,yl) benzene (TPBI) (QD/TPBI blend film), which is the core unit for the highly efficient quantum dot LEDs, was deposited on quartz substrates from QD and TPBI mixed solutions by a spin coater. The morphology of the Mn:ZnCdS samples were characterized by a transmission electron microscope (TEM) (JEM-2100F, JEOL, Japan). In the measurements of temperature dependent PL spectra and decay curves, the samples were prepared by dropping QDs dispersed in chloroform on silicon wafer substrates and mounted in a Janis VPF-800 vacuum liquid nitrogen cryostat during measurement in the range from 80 to 480 K. The PL spectra and PL decays were recorded using a Horiba Jobin Yvon Fluromax-4P with a time-correlated single-photon-counting (TCSPC) spectrometer. A 150-W ozone-free xenon arc-lamp was used as the continuous excitation source, and a pulsed xenon lamp was utilized as the excitation source for PL decay measurements. The PL QYs were recorded using a Horiba Jobin Yvon Fluromax-4P with Quantum-Yield accessory, which can obtain the absolute QY values. Relative to calculated by comparing the solution to an organic dye, the absolute PL QY measurement can effectively reduce the experimental error.

3. Results and Discussion

Figure 1 shows the temperature-dependent PL spectra of Mn:ZnCdS QDs recorded in the range from 80 to 480 K. The average diameters of the as-synthesized Mn:ZnCdS QDs and the QDs without

CdS shell overcoating (MnS/ZnS QDs) are *ca.* ~4.8 nm and ~2.8 nm, respectively (the inset in figure 1(a) and figure S1 in ESI†, respectively). Considering a thickness of 0.67 nm for 1 ML of the CdS shell

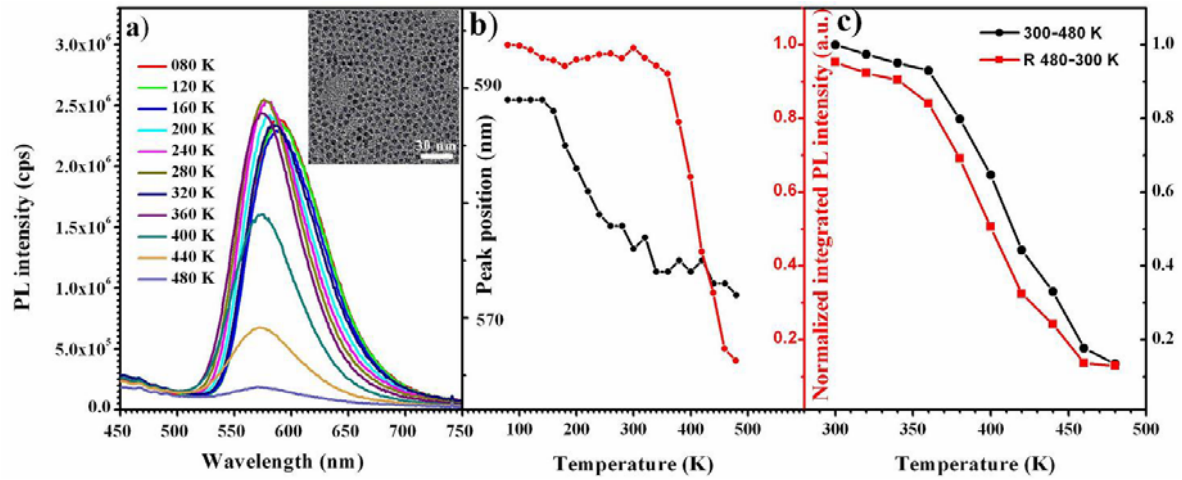

Figure 1. (a) The temperature-dependent PL spectra of Mn:ZnCdS QDs recorded in the range from 80 to 480 K. The inset shows the typical TEM image of the QDs. (b) PL peak positions (black line) and integrated intensities (red line) of the Mn^{2+} ion emission, (c) Temperature-dependent integrated PL intensities of Mn:ZnCdS QDs in heating-cooling cycle processes. The black and red lines refer to the heating and cooling processes, respectively.

in our case, the thickness of the CdS shell is estimated to be ~3.0 MLs. The Mn:ZnCdS QDs show a strong PL centered at ~570 to 590 nm when excited at 365 nm at various temperatures, which are confirmed to originate from a typical emission of Mn^{2+} ions due to its $^4T_1$ to $^6A_1$ transition.[37] The onset in the excitation spectra of the Mn^{2+} ion emission in the Mn:ZnCdS QDs is ~420 nm,[37] which is between that of MnS/ZnS (~325 nm)[13] and MnS/CdS QDs (~470 nm) with similar size, suggesting the formation of the ZnCdS alloy compound host, due to the interdiffusion of Zn and Cd ions over the high

temperature synthesis process. It means that, as compared to the Mn:ZnS QDs, Mn:ZnCdS counterparts have narrower band gap and more efficient absorption in the visible region. This could be a unique advantage to be utilized in the QD-sensitized solar cells and QD-LED devices. Figure 1(b) depicts the temperature dependence of the integrated PL intensities and the peak positions of Mn^{2+} ion luminescence. The integrated PL intensity almost keep constant when the temperature increases from 80 to 360 K (figure 1(b)), indicating that the PL QY of our Mn:ZnCdS QDs can keep up to ~65% even at a high temperature of 360 K (~70% at room temperature). The thermal stability of our Mn:ZnCdS QDs is superior than those of undoped QDs reported before, which generally exhibits a durative strong quenching of the luminescence intensity from lower temperatures to the elevated temperatures (*e.g.* CdSe/CdS/ZnS core/shell/shell QDs from 300 to 500 K,[26] CdTe QDs from 15 to 210 K,[39] and CdSe/ZnS core/shell QDs from 45 to 295 K[40]). This could be mainly ascribed to the thermally activated photoionization of the photoexcited carriers in QDs.[24] The PL intensity decreases rapidly with the increase of the temperature from 360 K and remains 14% of its initial value at 480 K. In order to know whether the quenching is intrinsic or not, the temperature-dependent PL spectra of Mn:ZnCdS QDs in heating-cooling cycle processes were recorded, and the corresponding integrated PL intensities were plotted in figure 1(c). It seems that the PL intensity almost fully recovers upon cooling (remains ~95% of its initial value), which suggests that the irreversible quenching process is absent. The reversible quenching suggests that the thermal quenching of the PL is intrinsic and the performance of the Mn:ZnCdS QDs can kept well even after high temperature treatment.[24] These results imply that the Mn^{2+} ions doped QDs are more robust than the undoped counterparts, which can meet the requirements for the applications in various functioning devices.

As shown in figure 1(b), the PL peak wavelength gradually shifts to a higher energy by 68 meV

(from 589 to 572 nm) when the temperature increases from 80 to 480 K. The blue shift of PL is generally attributed to the thermal expansion of the host lattice induced by the raise of the temperatures. [10,41,42] However, in our case, the observed blue shift (~68 meV) obviously shows a much stronger temperature dependence than those of Mn^{2+} ions doped ZnS or CdS QDs (almost ~5 fold larger[10]). Chen *et al* .[10] have studied the tunable temperature dependence of Mn^{2+} ions PL peak position in Mn^{2+} ions doped CdS/ZnS core/shell QDs, which suggested that the larger local lattice strain within the dopant site could cause a stronger temperature dependence of the luminescence peak, due to the enhanced local thermal expansion within the dopant site. In our case, for the as-synthesized Mn:ZnCdS QDs with a MnS/ZnS/CdS core-shell structure, although the localized nature of the Mn^{2+} ions is not very clear currently, there must be a local lattice strain within the dopant site since the CdS has a larger lattice parameter (5.82 Å) than ZnS (5.41 Å). [10] That is to say, the localized lattice strain within the Mn:ZnCdS QDs makes the enhanced blue shift of the PL.[10,22]

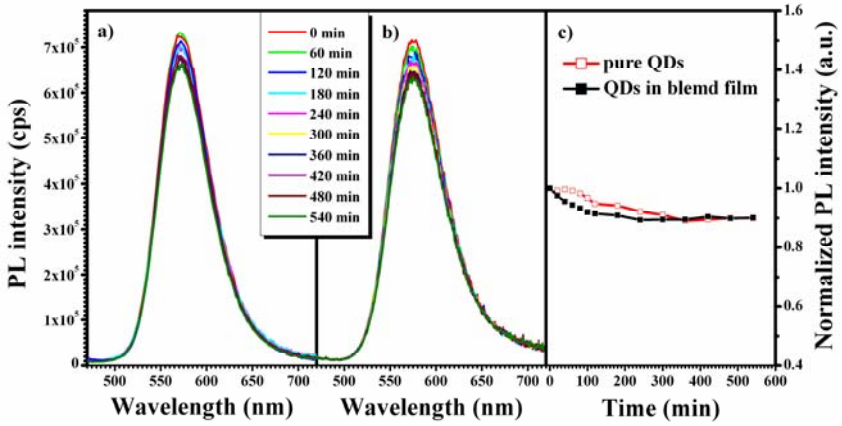

Figure 2. (a) The evolution of PL spectra of the close-packed Mn:ZnCdS QDs at 400 K. (b) The evolution of PL spectra of the QDs/TPBI blend film at 400 K. (c) The integrated PL intensities of Mn^{2+} ion emissions as a function of time.

For practical applications, besides the high PL QY, the thermal stability plays a critically important role for the QDs to be used in the device at an elevated temperature. Figure 2(a) and (b) show their PL spectra of the close-packed Mn:ZnCdS QDs and QDs/TPBI blend film during thermal treatment at 400 K for 540 minutes, respectively. It is found that the peak positions and contours of the PL spectra from both samples are almost identical, suggesting the invariability of the luminescence origin of Mn^{2+} ion emission. The PL intensities of the Mn:ZnCdS QDs decrease slightly and then keep constant with the increase of the time during the thermal treatment at 400 K (figure 2(c)). The PL intensities could remain ~90% as their initial values after the long high-temperature heat treatment at 400 K for 540 minutes, clearly suggesting the excellent high-temperature stability of our synthesized Mn:ZnCdS QDs.

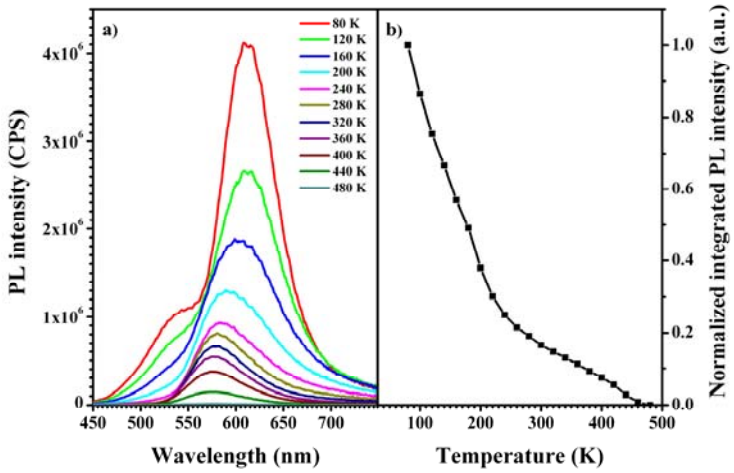

Figure 3. The temperature-dependent PL spectra (a) and integrated PL intensities (b) of Mn:ZnCdS QDs with a PL QY of 13% from 80 to 480 K. The integrated PL intensities are normalized to that measured at 80 K.

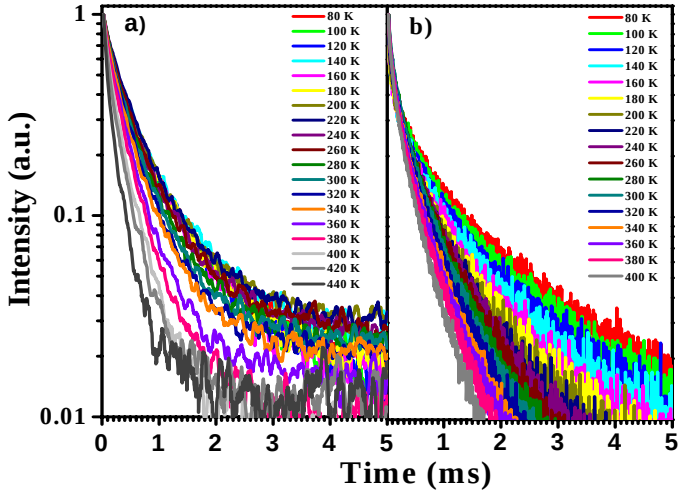

Figure 4. The temperature-dependent decay curves of Mn:ZnCdS QDs with a high PL QY of 70% (a) and low PL QY of 13% (b) from 80 to 440/400 K under the excitation at 365 nm, respectively.

To understand the thermal quenching mechanism, another sample of Mn:ZnCdS QDs with a low PL QY of 13%, which has the similar MnS core and ZnS buffer layer to the first sample and with a thin CdS shell (The representative synthesis procedure for the Mn:ZnCdS QDs, ESI†) were studied for comparison. The thickness of the CdS shell can be estimated to be ~1.0 MLs, since the size of the QDs is ~3.4nm (figure S1, ESI†). Their temperature-dependent integrated PL intensities are shown in figure 3. It seems that the Mn^{2+} ion emission intensity decreases quickly as the increase of the temperature from 80 to 480 K. There is ~88% loss in the PL intensity when heated up to 360 K as compared to that at 80 K, showing more sensitive to the temperature than that of the QDs with a thick shell (with a high PL QY). To better understand the different thermal quenching issues in the doped QDs with various shell thicknesses, the PL decay curves of Mn^{2+} ions are displayed in figure 4. The curves were fitted by

a bi-exponential function with two time components (τ_i) and weights (A_i). The amplitude-weighted lifetimes ($\tau_{Mn(T)}$) were obtained by a relation as bellow:

$$\tau_{Mn(T)} = (A_1\tau_1^2 + A_2\tau_2^2)/(A_1\tau_1 + A_2\tau_1) \text{.....(1)}$$

Consequently, the temperature-dependent integrated PL intensities and lifetimes are plotted in figure 5. The results demonstrate that the $\tau_{Mn(T)}$ exhibits a basically similar temperature-dependent trend as that of PL intensity ($I_{(T)}$) for the doped QDs with a high PL QY (figure 5(a)), implying the weak temperature-dependent efficiency of the energy transfer from the excitons to Mn^{2+} ions ($\Phi_{ET(T)}$) according to the equation of:

$$I_{(T)} \propto \Phi_{ET(T)} \times \Phi_{Mn(T)} \propto \Phi_{ET(T)} \times \tau_{Mn(T)} \text{.....(2)}$$

where $\Phi_{Mn(T)}$ is the efficiency of the Mn^{2+} ion emission. The weak temperature dependence of the $\Phi_{ET(T)}$ means the thermal quenching is mainly due to the decrease of $\Phi_{Mn(T)}$ at elevated temperature. Meanwhile, the PL intensity of the doped QDs with a low PL QY drops faster than the PL lifetime once the temperature over than 180 K(figure 5(b)), suggesting that both the decrease of $\Phi_{Mn(T)}$ and drop of $\Phi_{ET(T)}$ are responsible for the PL thermal quenching. The different quenching mechanisms in the doped QDs with various shell thickness might be attributed to the lower density of nonradiative recombination centers in the QDs with high PL QY and the larger energy transfer rate (~10^{11} s^{-1}) than Mn^{2+} ion radiative rate (10^3 s^{-1}). That is to say, the thermal stability of Mn^{2+} ion emission in QDs could be profoundly improved by increasing the shell thicknesses to decrease the density of nonradiative recombination centers.

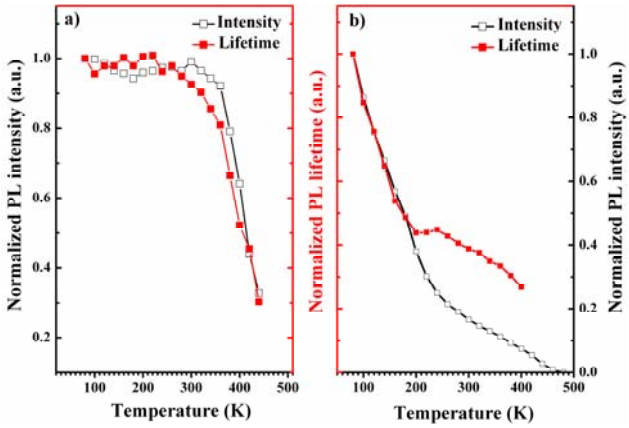

Figure 5. Temperature-dependent integrated PL intensities and average lifetimes of Mn:ZnCdS QDs with a high PL QY of 70% (a) and low PL QY of 13% (b). The integrated PL intensities and lifetimes are both normalized to those measured at 80 K.

It is generally considered that the elevated temperature could typically enhance the exciton-phonon coupling interactions in the host QDs for the doped QDs, which thus impact the energy transfer efficiency from the host to doped ions. Namely, the energy transfer from photoexcited exciton of the host to Mn^{2+} ions must compete with the nonradiative recombination resulting from exciton-phonon coupling interactions. Fortunately, the fast energy transfer rate (~10^{11} s^{-1})[43] and the low density of nonradiative recombination centers in our doped QDs with a high PL QY together allow them a weaker temperature-dependent energy transfer efficiency. Furthermore, the Mn^{2+} ions emission from the inner-core *d-d* transition ($^4T_1$ to $^6A_1$) in a tetrahedral coordination favors a less sensitivity to the environment.[44] Thus, as compared to the pristine counterparts, the QDs doped with Mn^{2+} ions could be expected to enhance their thermal stability.

4. Conclusions

In summary, we have demonstrated the thermal behaviors of Mn:ZnCdS QDs in the temperature range of 80-480 K. The PL QY of the as-synthesized QDs can keep up to 65% even at a high temperature of 360 K. Meanwhile, both close-packed QDs and QDs/organic blend films exhibit an excellent thermal stabilities at the elevated temperatures. The thermal stability of Mn^{2+} ion emission in QDs could be profoundly improved by increasing the shell thicknesses to decrease the density of nonradiative recombination centers. Current work might push forward the practical applications of the Mn^{2+} ions doped QDs in optical devices, especially for these to be worked in high temperature environments.

Acknowledgements

This work was financially supported by National Natural Science Foundation of China (NSFC, Grant No. 61106066), 973 Program (Grant No. 2012CB326407) and Zhejiang Provincial Science Foundation (Grant No. LY14F040001).

†Electronic Supplementary Information (ESI†) available: The representative synthesis procedure for the Mn:ZnCdS QDs; The typical TEM images for MnS/ZnS QDs without CdS shell and the Mn:ZnCdS QDs with thin shell thickness; Calculation of the ZnS buffer layer thicknesses; The PL quantum yield (QY) measurements.

References.

[1] A. Mews and J. Zhao, *Nat. Photonics,* 2007, **1**, 683.

[2] S. Coe, W.-K. Woo, M. G. Bawendi and V. Bulović, *Nature*, 2002, **420**, 800.

[3] Y. Shirasaki, G. J. Supran, M. G. Bawendi and V. Bulović, *Nat. Photonics,* 2012, **7**, 13.

[4] P. V. Kamat, *J. Phys. Chem. Lett.,* 2013, **4**, 908.

[5] W. Zhang, Q. Lou, W. Ji, J. Zhao and X. Zhong, *Chem. Mater.,* 2013, **26**, 1204.

[6] S. C. Erwin, L. Zu, M. I. Haftel, A. L. Efros, T. A. Kennedy and D. J. Norris, *Nature,* 2005, **436**, 91.

[7] N. Pradhan and X. Peng, *J. Am. Chem. Soc.,* 2007, **129**, 3339.

[8] H.-Y. Chen, T.-Y. Chen and D. H. Son, *J. Phys. Chem. C,* 2010, **114**, 4418.

[9] H.-Y. Chen, S. Maiti and D. H. Son, *ACS Nano,* 2012, **6**, 583.

[10] H.-Y. Chen, S. Maiti, C. A. Nelson, X. Y. Zhu and D. H. Son, *J. Phys. Chem. C,* 2012, **116**, 23838.

[11] S. Acharya, D. Sarma, N. R. Jana and N. Pradhan, *J. Phys. Chem. Lett.,* 2009, **1**, 485.

[12] S. Jana, B. B. Srivastava, S. Jana, R. Bose and N. Pradhan, *J. Phys. Chem. Lett.,* 2012, **3**, 2535.

[13] J. Zheng, X. Yuan, M. Ikezawa, P. Jing, X. Liu, Z. Zheng, X. Kong, J. Zhao and Y. Masumoto, *J. Phys. Chem. C,* 2009, **113**, 16969.

[14] S. Nizamoglu, T. Erdem, Xiao Wei Sun, and H. V. Demir, *Opt. Lett.,* 2010, **35**, 3372.

[15] P. Gu, Y. Zhang, Y. Feng, T. Zhang, H. Chu, T. Cui, Y. Wang, J. Zhao and W. W. Yu, *Nanoscale,* 2013, **5**, 10481.

[16] B. Lin, X. Yao, Y. Zhu, J. Shen, X. Yang, H. Jiang and X. Zhang, *New J. Chem.,* 2013, **37**, 3076.

[17] P. V. Kamat, *Acc. Chem. Res.,* 2012, **45**, 1906.

[18] J. Luo, H. Wei, Q. Huang, X. Hu, H. Zhao, R. Yu, D. Li, Y. Luo and Q. Meng, *Chem. Comm.,* 2013, **49**, 3881.

[19] R. Zeng, M. Rutherford, R. Xie, B. Zou and X. Peng, *Chem. Mater.,* 2010, **22**, 2107.

[20] J. Lin, Q. Zhang, L. Wang, X. Liu, W. Yan, T. Wu, X. Bu and P. Feng, *J. Am. Chem. Soc.,* 2014, **136**, 4769.

[21] F. Huang, J. Zhou, J. Xu and Y. Wang, *Nanoscale,* 2014, **6**, 2340.

[22] A. Hazarika, A. Layek, S. De, A. Nag, S. Debnath, P. Mahadevan, A. Chowdhury and D. Sarma, *Phys. Rev. Lett.,* 2013, **110**, 267401.

[23] R. Beaulac, P. I. Archer, X. Liu, S. Lee, G. M. Salley, M. Dobrowolska, J. K. Furdyna and D. R. Gamelin, *Nano Lett.,* 2008, **8**, 1197.

[24] V. A. Vlaskin, N. Janssen, J. V. Rijssel, R. Beaulac and D. R. Gamelin, *Nano Lett.,* 2010, **10**, 3670.

[25] C. E. Rowland, W. Liu, D. C. Hannah, M. K. Y. Chan, D. V. Talapin and R. D. Schaller, *ACS Nano,* 2014, **8**, 977.

[26] Y. Zhao, C. Riemersma, F. Pietra, R. Koole, C. M. Donega and A. Meijerink, *ACS Nano,* 2011, **6**, 9058.

[27] Q. Dai, Y. Song, D. Li, H. Chen, S. Kan, B. Zou, Y. Wang, Y. Deng, Y. Hou, S. Yu, L. Chen, B. Liu and G. Zou, *Chem. Phy. Lett.,* 2007, **439**, 65.

[28] I. J. Kramer and E. H. Sargent, *Chem. Rev.,* 2014, **114**, 863.

[29] N. D. Bronstein, L. Li, L. Xu, Y. Yao, V. E. Ferry, A. P. Alivisators and R. G. Nuzzo, *ACS Nano,* 2014, **8**, 44.

[30] X. Yuan, J. Zheng, R. Zeng, P. Jing, W. Ji, J. Zhao, W. Yang and H. Li, *Nanoscale,* 2014, **6**, 300.

[31] B. T. Diroll and C. B. Murray, *ACS Nano,* 2014. DOI:10.1021/nn5021314.

[32] D. Norris, N. Yao, F. Charnock and T. Kennedy, *Nano Lett.,* 2001, **1**, 3.

[33] M. Tanaka and Y. Masumoto, *Chem. Phys. Lett.,* 2000, **324**, 249.

[34] W. Chen, A. G. Joly, J.-O. Malm, J.-O. Bovin and S. Wang, *J. Phys. Chem. B,* 2003, **107**, 6544.

[35] W. Zhang, Y. Li, H. Zhang, X. Zhou and X. Zhong, *Inorg. Chem.,* 2011, **50**, 10432.

[36] R. Zeng, T. Zhang, G. Dai and B. Zou, *J. Phys. Chem. C,* 2011, **115**, 3005.

[37] S. Cao, J. Zheng, J. Zhao, L. Wang, F. Gao, G. Wei, R. Zeng, L. Tian and W. Yang, *J. Mater. Chem. C,* 2013, **1**, 2540.

[38] X. Yu, X. Peng, Z. Chen, C. Lian, X. Su, J. Li, M. Li, B. Liu and Q. Wang, *Appl. Phys. Lett.,* 2010, **96**, 123104.

[39] G. Morello, M. D. Giorgi, S. Kudera, L. Manna, R. Cingolani and M. Anni, *J. Phys. Chem. C,* 2007, **111**, 5846.

[40] D. Valerini, A. Creti, M. Lomascolo, L. Manna, R. Cingolani and M. Anni, *Phys. Rev. B,* 2005, **71**, 235409.

[41] J. Suyver, J. Kelly and A. Meijerink, *J. Lumin.,* 2003, **104**, 187.

[42] J. MacKay, W. Becker, J. Spaek and U. Debska, *Phys. Rev. B,* 1990, **42**, 1743.

[43] H. -Y. Chen and D. H. Son, *Isr. J. Chem.,* 2012, **52**, 1016.

[44] K. P. Kadlag, M. J. Rao and A. Nag, *J. Phys. Chem. Lett.,* 2013, **4**, 1676.